Detecting the Fetal Electrocardiogram by Wavelet Theory-Based Methods

F. MOCHIMARU, Y. FUJIMOTO

Department of Obstetrics and Gynecology, Hiratsuka City Hospital, Hiratsuka City, Japan

Y. ISHIKAWA

Ishikawa Medical Clinic, Saitama City, Japan

Summary

Accurate detection of fetal heart signals during pregnancy has the potential to provide specific information on possible fetal cardiac diseases. By analyzing standard ECG recordings derived from leads placed on the maternal abdomen, we determined that fetal signals have very low power relative to that of the maternal ECG, and they are mixed with several sources of interference. We took noninvasive fetal electrocardiograms from the maternal abdomen, extracted the fetal QRS complex, P wave and T wave from the maternal electrocardiogram waveforms, and identified the features of those waveforms. The waveform of the fetal ECG is morphologically similar to that of the adult ECG in the continuous wavelet transform, which is a method for analyzing time-dependent signals in both time and frequency domains. We showed that the observed waveforms were not noise, but were actually the fetal ECG. Our high-frequency, high-resolution ECG allows the fetal P wave and T wave to be monitored. We think this will become a powerful tool for diagnosing and treating fetal arrhythmias.

Key Words

Wavelet transforms, fetal ECG, wavelet-based detrending, wavelet-based denoising, Lipschitz exponents

Introduction

Just as an electrocardiogram is useful in diagnosing cardiac diseases in children and adults, the analysis of the fetal electrocardiogram (FECG) could be a reliable method for diagnosing cardiac diseases, especially fetal arrhythmias. During delivery, accurate recordings can be made by placing an electrode on the fetal scalp. However, during pregnancy other methods should be used due to the inaccessibility of the fetus. Ideally, the FECG recorded from the maternal abdomen is a highly desirable, noninvasive method. However, FECG signals have very low power relative to that of the maternal ECG (MECG) due to several sources of interference. Potential recordings taken on the maternal abdomen are affected not only by large baseline fluctuations (caused by several bioelectric phenomena), but also by various types of noise (intrinsic noise from

a recorder, noise from electrode-skin contact, etc.). This makes it difficult to discriminate between FECG waveforms and extraneous noise.

With large baseline fluctuations, we used wavelet-based multiresolution analysis (MRA) to exclude those trends. We also used MRA to remove noise. Furthermore, to prove that the observed waveforms were not due to noise but actually were FECG waveforms, we used the mathematical characterization of singularities with Lipschitz exponents.

While earlier researchers [1,2] studied only those peaks thought to be the fetal QRS complex, not the actual FECG waveforms, our technique allows all of the ECG waveforms to be observed, such as the P wave, QRS complex, and T wave. Through continuous waveform analysis (CWT) [1], i.e., analysis of the

time and frequency domain, the waveforms thought to be the acquired FECG showed a form very similar to that of adult ECG waveforms. Thereby, we have shown that the QRS complex under the CWT has a gourd shape. The main structural T4 component of the T wave is a horizontally elongated spindle shape at frequencies less than the low frequency part of the QRS complex, forming the base of the gourd shape. If the T wave is flattened and lowered, this base will exist directly under the QRS, and if the T wave is strong, it will be displaced after the QRS complex [3].

Materials and Methods

Maternal and Fetal ECG

Using the naked eye, it is almost impossible to recognize the admixture of the fetal ECG waveform in standard ECG leads from that of a pregnant woman. When performing a fetal ECG with the wrist leads placed over the maternal abdomen on both sides of the uterine fundus, the amplitude of the maternal QRS complex will be reduced by 90% compared to standard lead placement, and the fetal QRS will be easier to decipher. For the purposes of this paper, we positioned the leads as stated above. We used a high-frequency high-resolution ECG (HFHR-ECG) [3] with sampling rates from 5 to 20 kHz to store the time frames on a computer for further analysis. The FECG recordings were performed on a 27-year-old woman during the 38th week of pregnancy.

Continuous Wavelet Transformation

Wavelet theory is designed to provide good time resolution and poor frequency resolution at high frequencies, and good frequency resolution and poor time resolution at low frequencies. This approach is useful for ECG signals, i.e., signals, with high frequency components for short durations, and low frequency components for long durations. From a one-dimensional input signal $f(t)$, in this case the ECG signal, the continuous wavelet transformation is a two-dimensional function

$$CWT(a,b) = \frac{1}{\sqrt{a}} \int_{-\infty}^{+\infty} f(t) \; \Psi^* \left(\frac{t-b}{a} \right) dt$$

of a scale parameter ($a \sim 1/\text{frequency} > 0$) and a translation parameter ($b = $ time localization at which the signal is analyzed). There are several wavelet functions (mother wavelets $\mathbf{\Psi}(t)$ with $\mathbf{\Psi}^*(t)$ conjugate complex)

available with different properties. Here, Gabor-8 Power wavelets [4] were used as the maternal wavelets for the CWT.

Some other methods of wavelet analysis were used to check the results; the Daubechies method [5] was used for discrete wavelet transforms and the Wickerhauser methods [6] were used for wavelet packet transforms with the best basis algorithm. All analyses were performed using "Wavelet Analysis and Spectrum Analysis Software: MEM" [7].

Wavelet Transform Based Detrending

For this paper, detrending according to the Jensen method [8] was applied to data in which the samples had large baseline fluctuations. Therefore, we performed MRA up to the 12th level of the raw ECG data using Daubechies20 wavelets. The 12th order approximation function (f_{12}) consists of slow variations and was removed from the raw ECG for further data processing.

Wavelet Transform Based Noise Removal

There is no universal method to reduce noise. Because patterns of noise distribution (the probabilty distribution function of noise) are different, i.e., Gaussian distribution white noise, and uniform distribution white noise, denoising is always a trade-off [9]. Our ECG data with MRA show that there were several types of noise. To remove these noises, we applied wavelet transform-based denoising of the detrended data by multiresolution analysis up to the 12th levels using Coiflet24 wavelets.

Denoising was performed according to different criteria. In so called hard-thresholding, wavelet coefficients on some or all scales that are below a certain threshold are believed to be noise and they are set to zero. In so called soft -thresholding, additionally, coefficients on all coefficients above this threshold are reduced by the value of the threshold. Generally, we used the hard thresholding to remove noise, which localized some levels, and soft thresholding to remove the noise uniformly.Weighted standard deviations of the wavelet coefficients at each resolution level in MRA [7] were used as the thresholds at each resolution level. For example, if the standard deviation of the wavelet coefficient of level 7 is σ_7 and the weighting factor is s_7, the threshold is given by $\lambda_7 = \sigma_7 \times s_7$. We selected weighting factors which made the cost of the information-cost-function (e.g., information entropy, Gauss-Markov entropy, theoretical dimension [6,7]) as small

as possible, and also made the coefficient of determination (square of the correlation coefficient) as large as possible.

Lipschitz Exponents

We acquired the modulus maxima (local extrema) [10] from the fast dyadic transformation of the denoised ECG signal by using the quadratic spline wavelet of Mallat [4] and Carmona et al. [11]. Although only the maxima are determined by this method, since the fetal and maternal QRS have opposite orientations, we also determined the minima, and took the vertical direction into consideration. In the following, the Lipschitz exponent is calculated from the decay of the modulus maxima amplitude by the slope of the decay curve less 0.5 [4]. Although this method has a poor frequency resolution, it is excellent for detecting fractal structure and singularities; a singularity with a Lipschitz exponent < 0 is believed to be related to noise. However, if there are high-power peaks, such as the maternal QRS and maternal T wave present in the vicinity of the fetal ECG waveform, the fetal waveform will be influenced and the Lipschitz exponents and other aspects will change as well. Thus, the modulus maxima technique is not suited for detecting complex morphological characteristics.

Results

Wavelet Transform-Based Detrending

A typical maternal ECG from the second limb lead that includes the fetal ECG is superimposed on slow variations (Figure 1a), which are removed by applying multiresolution analysis (Figure 1b).
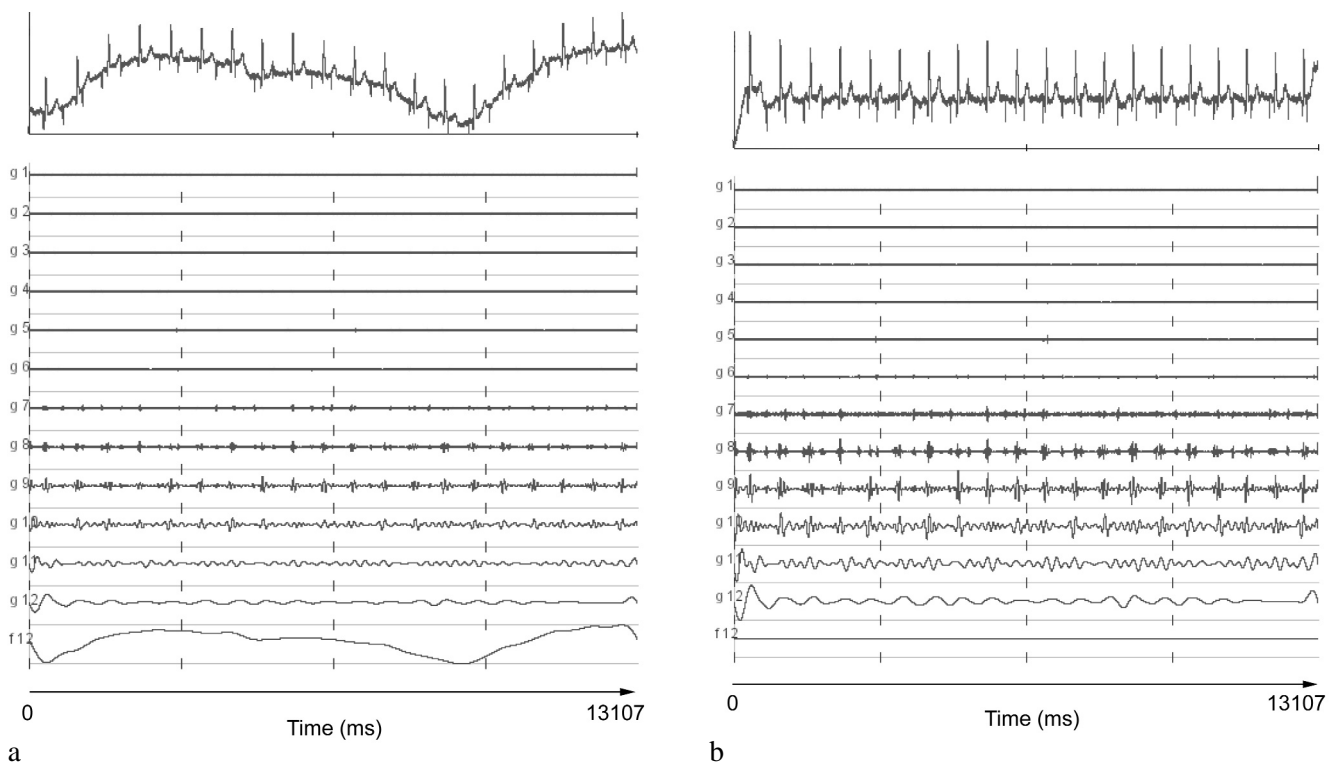

Figure 1. Maternal ECG (modified lead II, sampling rate 10 kHz) that includes the fetal ECG (38th week of pregnancy). The maternal heart rate was 92 beats/min and the fetal heart rate was 143 beats/min.
Panel a) Multiresolution analysis with Daubechies20 wavelet before detrending. The 12th order approximation function f_{12} (with $f_{j-1} = f_j + g_j$) is thought to consist of slow variations.
Panel b) The Multi resolution analysis of the data after detrending, i.e., after removal of f_{12} from the raw ECG signal. This post-detrending ECG shows no baseline fluctuations. Also note that f_{12} is essentially flat.
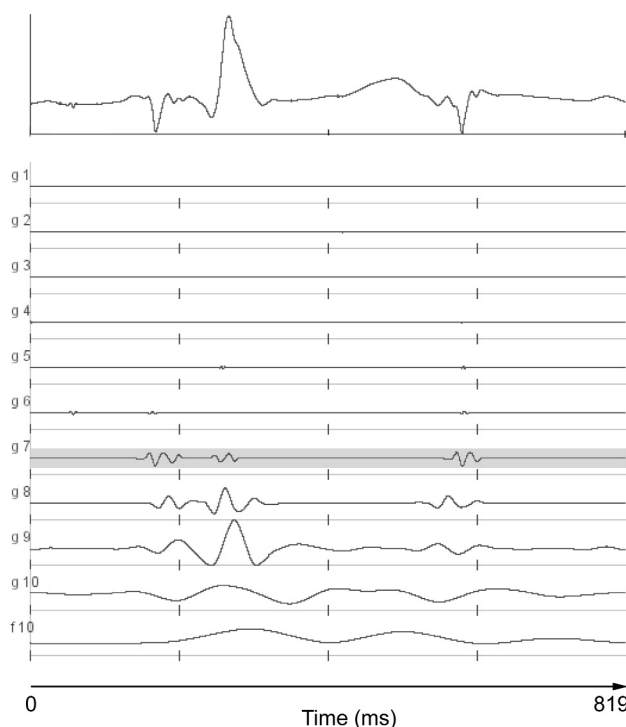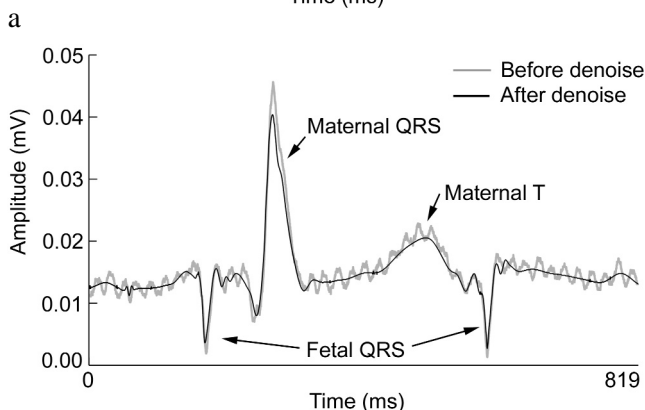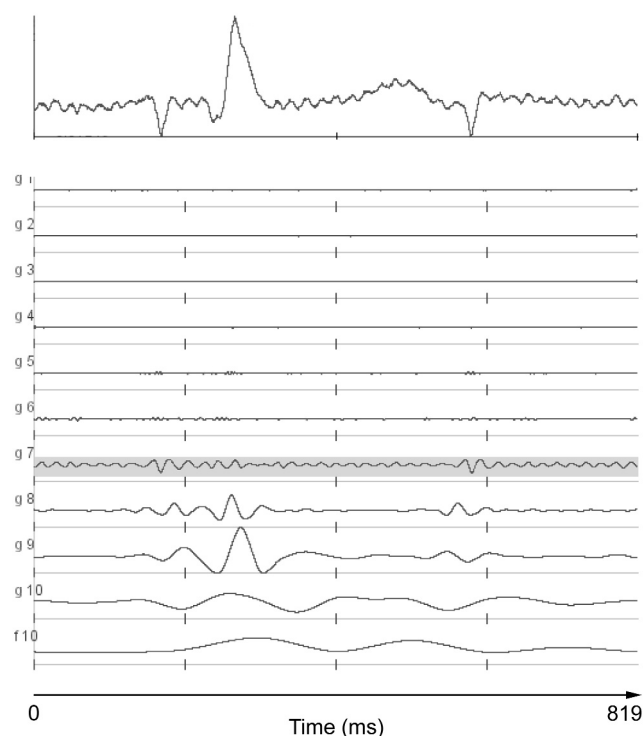
a

b

c

Figure 2. Denoising of a portion of Figure 1b.
Panel a) Multiresolution analysis with Coiflet24 wavelets. Large amounts of noise are seen at level 7 and below. We removed this noise by using indices such as the coefficient of determination and information cost functions, and used the standard deviation of the wavelet coefficients for each level as threshold weighting factors. We used weighting factors of 4.0 times the standard deviation for levels 1 to 3, 2.5 times the standard deviation for levels 4 and 5, 2.0 times for level 6, 1.5 times for level 7, and 0.6 times for level 8 (coefficient of determination $RR^2 = 0.976$, information entropy = 16.69, theoretical dimension = 12387).
Panel b) Multiresolution analysis with Coiflet24 wavelets after hard-threshold denoising. The noise at the g_7 level is reduced and wave motion is only visible at the locations of the maternal and the fetal QRS complex (information entropy =16.28 and theoretical dimension = 12014 were lower than before).
Panel c) Comparison of signals before and after Coiflet24 denoising. The light gray line is the signal before denoising, and the thick black line is the signal after denoising. Note that the direction of the fetal QRS complex is opposite that of the maternal QRS. The heavy line is the post-denoising data and the light gray line is the pre-denoising data.

Wavelet Transform-Based Denoising
The ECG waveform is shown in Figures 2 a,b, and c before and after denoising. The orientation of the fetal QRS is the opposite of the maternal QRS; this indicates that when the fetus is in the normal position in the uterus, the orientation of the fetal heart is opposite that of the maternal heart. High levels of noise are seen in the data under the eighth level, and the data under the third level is thought to be meaningless (no effect is seen in the CWT).
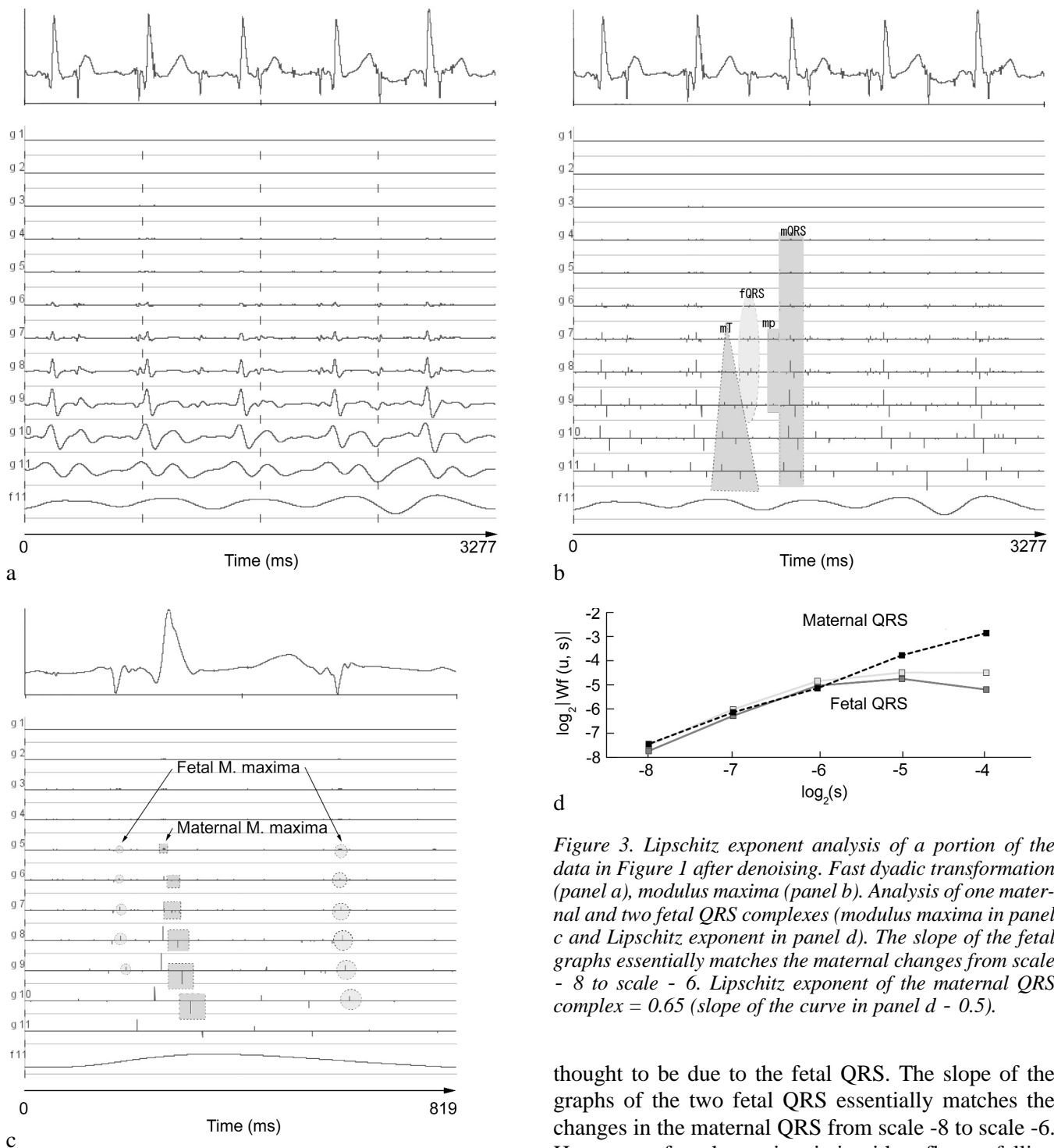
a

b

c

d

Figure 3. Lipschitz exponent analysis of a portion of the data in Figure 1 after denoising. Fast dyadic transformation (panel a), modulus maxima (panel b). Analysis of one maternal and two fetal QRS complexes (modulus maxima in panel c and Lipschitz exponent in panel d). The slope of the fetal graphs essentially matches the maternal changes from scale - 8 to scale - 6. Lipschitz exponent of the maternal QRS complex = 0.65 (slope of the curve in panel d - 0.5).

Lipschitz Exponents

Figure 3 shows the fast dyadic transformation and the modulus maxima of the denoised ECG. The sections enclosed in broken squares are peaks due to the maternal QRS and the sections enclosed in broken circles are thought to be due to the fetal QRS. The slope of the graphs of the two fetal QRS essentially matches the changes in the maternal QRS from scale -8 to scale -6. However, after that point, it is either flat or falling slightly. Noise by definition is localized and, thus, a singularity caused by noise does not have a long-term range. Consequently, the two small peaks in the ECG of Figure 3c, which have a singularity similar to the maternal QRS complex, are not noise but the fetal QRS complexes.
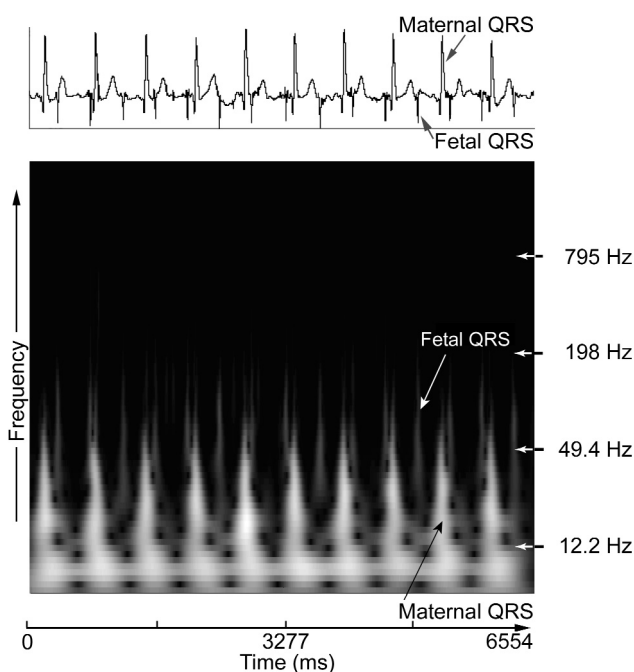
Figure 4. ECG (modified lead II) and continuous wavelet transform using Gabor 8 Power wavelets. The QRS complex in the maternal ECG waveform has a narrow, elongated gourd shape, and the fetal QRS complex has a narrow, elongated tear shape.
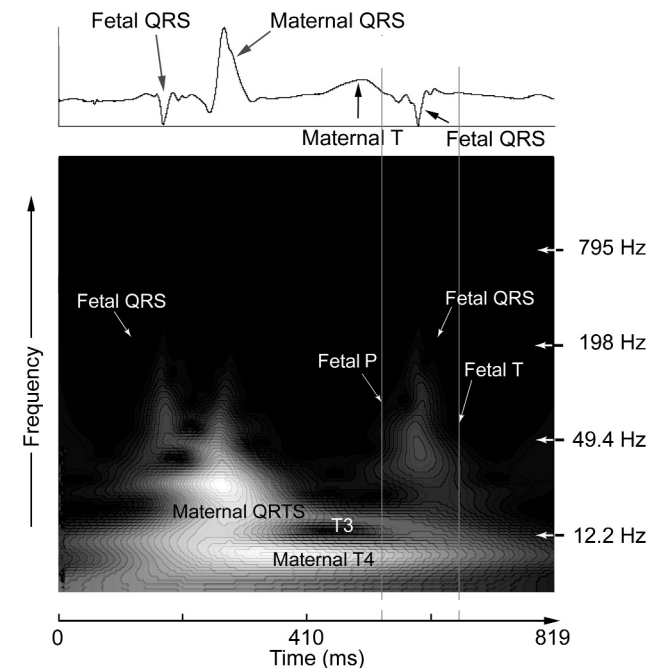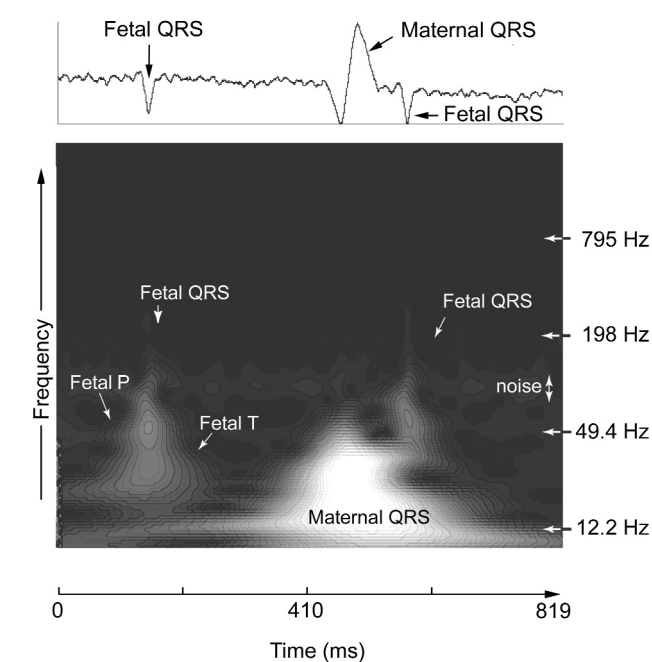

Figure 5. ECG (data of Figure 2c after denoising) and continuous wavelet transform using Gabor 8 Power wavelets. The maternal QRS complex and the main structural components (T3 and T4) of the maternal T wave are clearly seen. The second fetal ECG waveform, which is not affected by the maternal QRS complex, is typical for continuous wavelet transform and the positions of the fetal P wave and fetal T wave can be inferred from the image.

Fetal ECG

The maternal QRS complexes in Figure 4 have a narrow, elongated gourd shape. The fetal QRS complexes are shifted to higher frequencies and have a narrow, elongated tear shape. In maximum resolution CWT (Figure 5), the fetal QRS complexes have gourd-shaped features too and knots corresponding to the P wave and the T wave that can be seen in the CWT of typical ECGs [3].

To show the effect of noise, CWT of the raw ECG before denoising is performed. In Figure 6a, fetal P wave and fetal T wave can be recognized, as well as the fetal QRS. Since the fetal QRS on the right is close to the maternal QRS at the center of the figure, they influence each other and the shape is deformed relative to the typical form [3]. Noise is visible as horizontal frequency band between 50 and 200 Hz. In addition to a contour plot, the CWT is shown as a three-dimensional CWT image (Figure 6b). We can infer that the fetal P wave and fetal T wave can be seen in the fetal QRS complex at the left of the image: If it were possi-

ble to remove the noise in the vicinity of the fetal P wave, we might be able to extrapolate even more structural details.
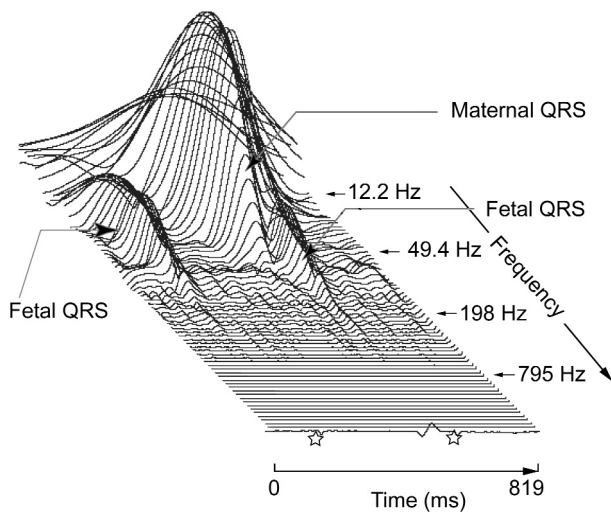
We performed hard denoising on the data from Figure 6. The CWT after denoising (Figures 7) are quite similar. The positions of the fetal P wave and fetal T wave can be inferred from the morphological features of the CWT [3] of the fetal ECG. By taking the projection of this positions (i.e., by drawing vertical lines in the CWT image), we can determine the position of the fetal P wave and fetal T wave in the raw ECG.

Superposition of the Fetal and Maternal QRS Complexes

We investigated techniques for detecting the combination of the fetal, with the maternal QRS complex. A special situation occurs for the fetal QRS complex superimposed by the maternal QRS complex (Figure 8a). As a result, the q and s lines that can be seen in a typical CWT [3] are not visible, and the ends are rounded. However, it is not clear whether or not the form of the
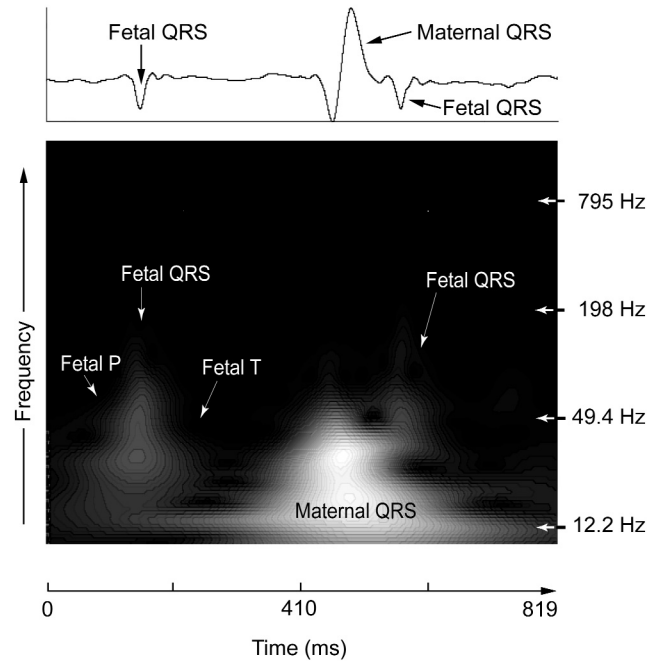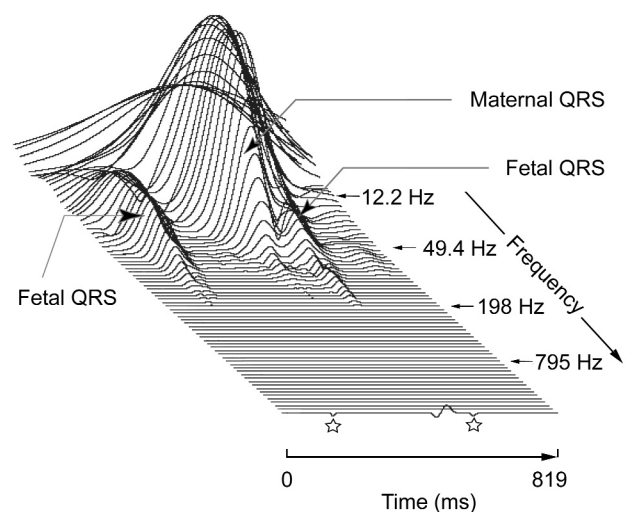
Figure 6. Pre-denoising raw ECG (modified lead aVF) and continuous wavelet transform using Gabor 8 Power wavelets. From the contour plot (panel a), the fetal ECG waveform is a typical ECG waveform after CWT, and thus, the positions of the fetal P wave and fetal T wave can be inferred [3]. The features of the other fetal ECG waveforms are similar. From the three-dimensional image, while we can infer that the fetal P and T wave can be seen in the fetal QRS complex at the left of the image and we could hope to extrapolate even more structural detail assuming we were able to remove the noise close to the fetal P wave.

Figure 7. Post-denoising ECG (modified lead aVF) and continuous wavelet transform using Gabor 8 Power wavelets shown as a contour plot (panel a) and three-dimensional image (panel b). Compared to the pre-denoising data (Figure 6), the noise in the range shown by the arrows at the ends of the graph has been largely removed. We used indices such as the coefficient of determination and information cost functions, and used the standard deviation of the wavelet coefficients for each level as threshold weighting factor (coefficient of determination RR^2 = 0.964, information entropy = 1.46, theoretical dimension = 867, and Gauss-Markov entropy = -114454).
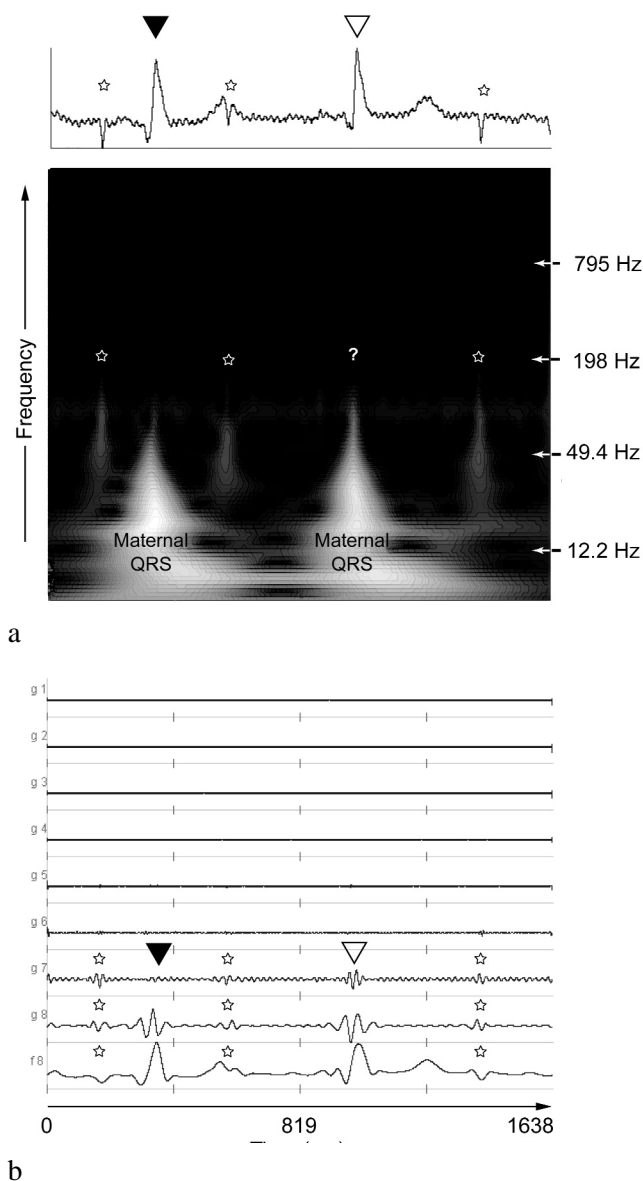
a

b

Figure 8. Pre-denoising ECG (modified lead II) which includes the maternal QRS complex (▼), fetal QRS complex (☆), and maternal QRS complex (▽) superimposed with a fetal QRS complex (?).
Panel a) Continuous wavelet transform using Gabor 8 Power wavelets. As a result of the superposition of the fetal and maternal QRS complex, the q and s lines (high frequency parts of the maternal QRS complex) that can be seen in a typical CWT example are not visible, and the ends are rounded.
Panel b) Multi resolution analysis using Coiflet24 wavelets up to a maximum resolution level of 8. The superposition of the fetal and maternal QRS complex on the g_7 level (▽) shows a large wave motion unlike the maternal QRS complex without a superimposed fetal QRS complex (▼).

maternal QRS complex has been changed by the overlapping fetal QRS complex. Therefore, we studied the changes in the form of the maternal QRS complex under multiresolution analysis with Coiflet24 wavelets according to whether or not an added fetal QRS complex is present (Figure 8b). The section believed to be superposed by the fetal QRS complex has a large wave motion, which is not seen in the section without a superposed fetal QRS complex. If we consider this in conjunction with the fact that fetal QRS wave motion appears in the vicinity of g_7, g_8, and f_8, this can be seen as proof of the superimposition of the fetal QRS complex on the maternal QRS complex. Similar phenomena were observed using Daubechies20 and Spline24 wavelets as well.

Discussion

In order to fully exhibit its capabilities, high-frequency sampling is necessary to provide wavelet transform; this has been described as a mathematical microscope for the natural sciences. The sampling frequency used in conventional ECGs is 250 Hz (which is close to a resolution of 1 Byte/s = 2^8 /s = 256 /s). If orthonormal wavelets are used and we assume that we will use a number of wavelet coefficients up to the number that has meaning for multiresolution analysis, then we can only perform analysis up to 8 levels for Haar wavelets and up to 4 levels for Daubechies 20 wavelets. Khamene et al. [2] acquired fetal ECGs at 500 Hz from the maternal abdomen, and performed wavelet analyses using the modulus maxima. However, even if the modulus maxima (the quadratic spline wavelets) are used, this is not an adequate sampling frequency to extract the singular points or to calculate the Lipschitz exponent, which expresses the characteristics of the singular points. Mallat [4] starts the Lipschitz exponent calculation from scale 3, where distortion in the vertical direction becomes smaller. Therefore, at 500 Hz the maximum scale that can be used for the calculation is 5 and no one can guarantee that the local maxima of the fetal and maternal QRS complexes remain within the range of these scales. In the Khamene et al. [2] paper, the analysis with the modulus maxima was limited to scale 5, and they did not actually calculate the Lipschitz exponent. Furthermore, to perform multiresolution analysis for many wavelets, meaningful analyses at 500 Hz are limited to 4 levels, or at the most 5 levels, due to the number of wavelet coefficients. It

is difficult to fully extract the information and characteristics from a fetal ECG in an analyses which uses these insufficient scales (sampling rate at 500 Hz). Actually, their analysis does not identify the FECG P wave and T wave; it even has problems in discriminating the FECG-QRS complex from noise.

In our experience, the FECG-QRS will be obscured in the QRS of the MECG two or three times in a 10 seconds period, and it is difficult to extract the fetal QRS obscured in the maternal QRS with the modulus maxima or fast dyadic wavelet transformation. To demonstrate that the acquired ECG waveform includes the FECG waveforms and that those signals are not noise but are the FECG P wave, QRS complex and T wave, we performed the following functions. We calculated the Lipschitz exponent, analyzed the morphological features of the FECG using the continuous wavelet transform, and performed a wavelet packet analysis using a best basis algorithm with information entropy as the cost.

Conclusion

Analysis of the FECG could be a reliable method for diagnosing cardiac diseases, especially fetal arrhythmias. The HFHR-ECG can be noninvasively recorded from the maternal abdomen and allows the fetal P wave, QRS complex and T wave to be monitored. We believe that it will become a powerful tool for diagnosis and treatment of fetal arrhythmias.

References

[1] Kantz H, Schreiber T. Nonlinear time series analysis. Cambridge: Cambridge University Press, 1997: 168-171.

[2] Khamene A, Negahdaripour S. A new method for the extraction of fetal ECG from the composite abdominal signal. IEEE Trans Biomed Eng. 2000; 47: 507-516.

[3] Ishikawa Y, Mochimaru F. Wavelet theory-based analysis of high-frequency, high-resolution electrocardiograms: a new concept for clinical uses. Prog Biomed Res. 2002; 7: 179-184.

[4] Mallat S. Wavelet Tour of Signal Processing, 2nd edition. San Diego: Academic Press. 1998: 163-219, 249-254.

[5] Daubechies I. Ten Lectures on Wavelets. Philadelphia: SIAM Press. 1992: 195.

[6] Wickerhauser MV. Adapted Wavelet Analysis from Theory to Software. Natick: AK Peters. 1994: 273-298.

[7] Ishikawa Y. Wavelet Analysis for Clinical Medicine (in Japanese) with MEM Software on CD-ROM. Tokyo: Medical Publication (IGAKU-SHUPPAN). 2000: 154-163, 305-308.

[8] Jensen A, La Cour-Harbo A. Ripples in Mathematics. Berlin: Springer. 2000: 25-35.

[9] Jansen M. Noise Reduction by Wavelet Thresholding. New York: Springer. 2000: 35-45.

[10] Da Fontoura Costa F, Cesar RM Jr. Shape Analysis and Classification. New York: CRC Press. 2000: 502-524.

[11] Carmona R, Hwang W-L, Torresani B, et al. Practical Time-Frequency Analysis. Gabor and Wavelet Transforms with an Implementation in S (Wavelet Analysis and its Applications, Volume 9). San Diego: Academic Press. 1998: 206-215.

Contact
Fumio Mochimaru, MD
Department of Obstetrics and Gynecology
Hiratsuka City Hospital
1-19-1 Minamihara, Hiratsuka City, Kanagawa
Japan
Telephone: +81 463 32 0015
Fax: +81 463 31 4585
E-mail: KamaMF2169@aol.com